JoS JOURNAL OF STROKE

Journal of Stroke 2015;17(3):238-255
http://dx.doi.org/10.5853/jos.2015.17.3.238

Review

Vessel Wall Imaging of the Intracranial and Cervical Carotid Arteries

Young Jun Choi, Seung Chai Jung, Deok Hee Lee

Department of Radiology and Research Institute of Radiology, University of Ulsan College of Medicine, Asan Medical Center, Seoul, Korea

Vessel wall imaging can depict the morphologies of atherosclerotic plaques, arterial walls, and surrounding structures in the intracranial and cervical carotid arteries beyond the simple luminal changes that can be observed with traditional luminal evaluation. Differentiating vulnerable from stable plaques and characterizing atherosclerotic plaques are vital parts of the early diagnosis, prevention, and treatment of stroke and the neurological adverse effects of atherosclerosis. Various techniques for vessel wall imaging have been developed and introduced to differentiate and analyze atherosclerotic plaques in the cervical carotid artery. High-resolution magnetic resonance imaging (HR-MRI) is the most important and popular vessel wall imaging technique for directly evaluating the vascular wall and intracranial artery disease. Intracranial artery atherosclerosis, dissection, moyamoya disease, vasculitis, and reversible cerebral vasoconstriction syndrome can also be diagnosed and differentiated by using HR-MRI. Here, we review the radiologic features of intracranial artery disease and cervical carotid artery atherosclerosis on HR-MRI and various other vessel wall imaging techniques (e.g., ultrasound, computed tomography, magnetic resonance, and positron emission tomography-computed tomography).

Keywords Vessel wall imaging; Intracranial artery; Cervical carotid artery; High-resolution magnetic resonance

Correspondence: Seung Chai Jung
Assistant Professor, Department of Radiology and Research Institute of Radiology University of Ulsan College of Medicine, Asan Medical Center,
88 Olympic-ro 43-gil, Songpa-gu,
Seoul 05505, Korea
Tel: +82-2-3010-4355
Fax: +82-2-476-4719
E-mail: dynamics79@gmail.com

Received: April 4, 2015
Revised: August 19, 2015
Accepted: August 31, 2015

The authors have no financial conflicts of interest.

Introduction

Ischemic stroke caused by cerebrovascular disease is a major cause of mortality and morbidity worldwide, and the noninvasive *in vivo* assessment of plaques and arterial walls is a fundamental aspect in guiding therapy.[1-3] Luminal evaluation is the traditional method for evaluating and understanding vascular pathology. Although this evaluation is still one of the most important methods for assessing intracranial and carotid artery disease, it is limited in comparison with advanced imaging techniques. Vessel wall imaging—including magnetic resonance imaging (MRI), computed tomography (CT), and ultrasound (US) with color Doppler—can assess the morphology of atherosclerotic plaques, arterial walls, and surrounding structures in the cervical carotid artery. For a successful imaging of the vessel wall, an appropriate resolution for depicting the target vessel wall, a transverse imaging plane perpendicular to the long axis of the vessels,[4] and sufficient image contrast to characterize or differentiate the components of the vessel wall are necessary. High-resolution magnetic resonance imaging (HR-MRI) for vessel wall imaging usually consists of T1-/T2-weighted imaging, proton-density imaging, or contrast-enhanced T1-weighted imaging with turbo/fast spin-echo sequences or black-blood techniques.[4-6] Double inversion recovery and motion-sensitized driven equilibrium

are representative black-blood techniques.[4] Double inversion recovery is usually used with two-dimensional (2D) spin-echo or turbo/fast spin-echo sequences because of the single-slice sequential acquisition, which leads to the disadvantages of limited spatial resolution, a long scan time, and partial volume effects despite the effective suppression of blood signal.[7,8] Motion-sensitized driven equilibrium prepulses have recently been used in 3D HR-MRI by applying gradients along each axis. Radiofrequency pulses with flip angles of 90° and 180° are used for the preparative pulse before turbo/fast spin-echo sequences, and have the advantages of a shorter preparation time and larger coverage than double inversion recovery; however, this can lead to signal loss during the preparation time, susceptibility to field inhomogeneity, and incomplete suppression of blood or cerebrospinal fluid signals.[4,7,9] Vessel wall imaging can be used to assess various vascular pathologies other than atherosclerosis. When assessing intracranial artery disease, HR-MRI is one of the most important and popular vessel wall imaging techniques for directly evaluating the vascular wall. HR-MRI for intracranial vessel walls has generally involved the use of a resolution of < 1 mm (0.2-0.9 mm in 1.5-3 T MRI), a 2D or reconstructed 3D transverse imaging plane perpendicular to the arterial course,[4] and the black-blood technique in order to suppress the arterial blood or cerebrospinal fluid signals.[4,5] Intracranial artery atherosclerosis, dissection, moyamoya disease, vasculitis, and reversible cerebral vasoconstriction syndrome (RCVS) can be diagnosed and differentiated by using HR-MRI. Vessel wall imaging is expected to enhance the diagnostic performance of evaluations and the understanding of disease pathophysiology.[6,10-12]

The aim of this article is to (i) comprehensively review the use of HR-MR vessel wall imaging to assess intracranial artery disease, including atherosclerosis, dissection, moyamoya disease, vasculitis, and RCVS, and (ii) provide an overview of various vessel wall imaging techniques for the assessment of cervical carotid artery atherosclerosis, with specific emphasis on detection, analysis, and characterization.

HR-MRI for intracranial artery disease

Intracranial atherosclerosis

Ischemic stroke and intracranial artery disease demonstrate different characteristics depending on the race and region of the patient population. Intracranial atherosclerosis causes < 10% of ischemic strokes in white North American patients,[13,14] but causes 50%-60% of strokes in Asian populations.[15,16] Hispanic and black patients demonstrate a relative rate of intracranial atherosclerosis-related strokes that is five times greater than that of white patients.[17] Hence, the most common cause of ischemic stroke worldwide could be intracranial atherosclerosis.[16] Atherosclerosis results from a cascade of endothelial dysfunction processes, infiltration of modified lipids into the intima, and vascular wall inflammation or remodeling.[18] On HR-MRI, atherosclerotic plaques, lipid cores, fibrous components, hemorrhage, and calcium are the most important components.[6] In the cervical carotid arteries, it may be easier to characterize the vascular wall, to differentiate these components, and to diagnose the vascular pathology than in intracranial arteries, by using HR-MRI, owing to the larger size of the vessels. Vulnerable plaques can be differentiated from stable plaques according to the proportion or presence of plaque components.[6,19-21] However, HR-MR may be unable to characterize intracranial plaques in detail because of their small size and limited resolution (anterior cerebral artery, 2-3 mm; middle cerebral artery, 3-5 mm; posterior cerebral artery, 2-3 mm).[22,23] Although 3-T and 3D HR-MR were recently developed and can depict the isotropic voxel (0.4 × 0.4 × 0.4 mm) in clinical settings,[24] it is not necessarily easy to completely depict the components of atherosclerotic plaques.

Intraplaque hemorrhage on T1-weighted imaging and plaque enhancement on contrast-enhanced T1-weighted imaging are considered the most important factors in characterizing intracranial atherosclerosis. Intraplaque hemorrhage appears as a bright high-signal intensity on T1-weighted images according to a few histopathological[25] and radiological studies[26,27] of intracranial arteries, in addition to extrapolations from the cervical carotid artery.[28,29] A bright high-signal intensity is > 1.5 times brighter than the signal intensity of adjacent muscles,[27,29,30] which can suggest recent or fresh hemorrhage in cervical carotid atherosclerotic plaques.[6,29] However, this may still be insufficient evidence to show that all instances of intraplaque hemorrhage present as a bright high-signal intensity on T1-weighted images, or that the bright high-signal intensity of the intraplaque hemorrhage can be applied to various T1-weighted sequences. On cervical carotid artery imaging, there are also differences in signal intensities on the T1-weighted sequences.[31] Therefore, the detection and differentiation of intraplaque hemorrhage should be carefully performed by using various signal intensities. T2-weighted imaging or susceptibility on weighted imaging is also helpful.[32,33] Intraplaque hemorrhage is also associated with infarction in 30.4% of patients; however, intraplaque hemorrhage is not associated with infarction in 15.4% of patients according to a postmortem study.[34] Intraplaque hemorrhage, which is defined as a bright high-signal intensity on HR-MR, is significantly associated with ipsilateral stroke.[27]

Although the lipid core, fibrous component, and calcification in intracranial plaques cannot be sufficiently differentiated on HR-MRI, the HR-MR characteristics of these components seem

to be consistent with those of cervical carotid artery plaques.[35] The lipid core appears as an isointense area on T1-weighted images and as a hypo- to isointense area on T2-weighted images; the fibrous component appears as an isointense area on T1- and T2-weighted images; and calcification appears as an area of dark signal intensity on T1- and T2-weighted images.[35]

Plaque enhancement is the most common and reliable finding, which depends on T1-weighted imaging with gadolinium-based contrast enhancement. However, normal periarterial enhancement in the meninges or periarterial veins can disrupt the detection of true vascular wall enhancement.[36] Therefore, 3D HR-MRI may be more useful for differentiating pseudo-vessel wall components or for pseudo-enhancement in the intracranial arteries because it can show multiple imaging planes, including the perpendicular to arterial longitudinal axis. Plaque enhancement is also associated with recent ischemic stroke. Strong enhancement tends to indicate a short time interval from the onset of ischemic stroke to severe inflammatory activity.[24,37,38] Symptomatic plaques (63%) demonstrate a higher proportion of contrast enhancement than asymptomatic plaques (23%).[38] The degree of contrast enhancement decreases in symptomatic plaques over time (acute, 4 weeks; subacute, 4-12 weeks; chronic, > 12 weeks).[37] In ischemic stroke, the degree of enhancement may identify culprit plaques.[24] Plaque enhancement on HR-MRI has been explained as neovascularization or increased endothelial permeability.[39,40] Vessel wall enhancement may also occur in generalized inflammatory diseases, as well as in atherosclerotic plaques.[4] Therefore, arterial wall enhancement in equivocally suspected intracranial atherosclerosis cannot be conclusively excluded as another inflammatory vascular pathology.

Atherosclerotic plaque in the middle cerebral artery seems to be located predominantly in the opposite side as the orifices of perforators such as the coronary artery. In a stenotic middle cerebral artery, regardless of the symptoms, the plaque is distributed in the ventral and inferior wall more than in the superior and dorsal wall. However, symptomatic middle cerebral artery stenosis shows more superior wall plaque, which may be associated with perforators arising from the superior and dorsal wall of the middle cerebral artery.[41]

The shape of any thickened vessel wall (or plaque) can play an important role in differential diagnosis. Atherosclerotic plaques tend to appear as asymmetrically thickened walls—so-called eccentricity—relative to other vascular pathologies.[42] Quantitative measurement and analysis of the plaque shape is increasingly more convenient and reliable owing to the development of HR-MR. The eccentricity index is calculated by using the following formula: (maximal thickness-minimal thickness)/maximal thickness. If the index is ≥ 0.5, the area is defined as an eccentric plaque.[43] Positive and negative remodeling are also important characteristics that are extrapolated from coronary atherosclerosis.[44] Positive remodeling may also be associated with symptomatic plaques.[45,46] The remodeling index is calculated by using the following formula: maximum outer wall area/([proximal normal arterial area + distal normal arterial area]/2). If the index is ≥ 1.0, the area is defined as positive remodeling; otherwise, the area is defined as negative remodeling[47,48] (Figures 1 and 2). Intraplaque hemorrhage and strong contrast enhancement can be associated with vulnerable plaques in intracranial atherosclerosis, and the distribution, eccentricity, and remodeling characteristics may help depict atherosclerosis (Table 1).

Intracranial artery dissection

Intracranial artery dissection is an important cause of ischemic stroke in young adults (i.e., age 20-50 years).[12] Ischemic symp-

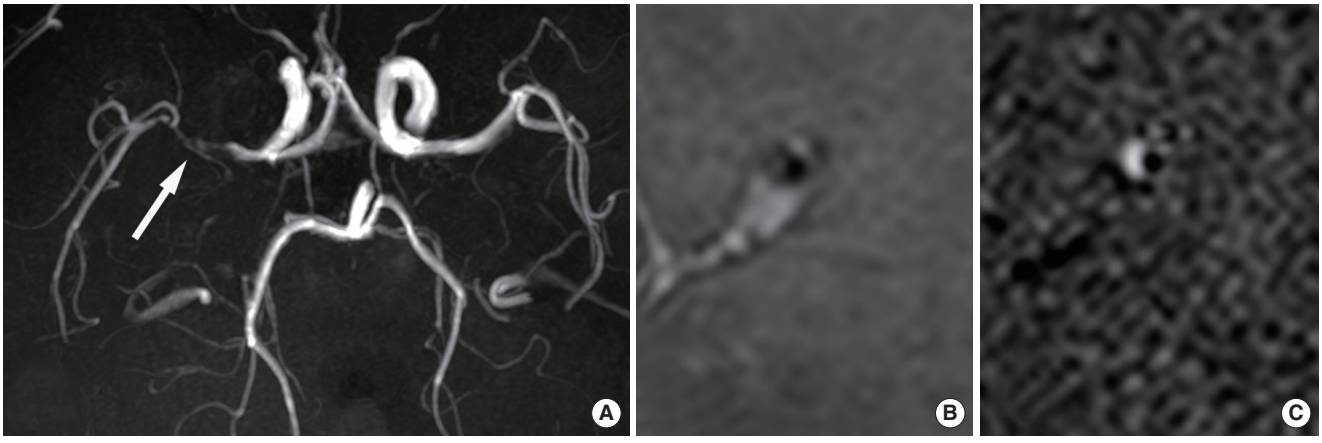

Figure 1. Intracranial atherosclerosis. A 49-year-old female patient presented with left-side weakness and four atherosclerotic risk factors. (A) Time-of-flight magnetic resonance angiograph showing severe stenosis in the right middle cerebral artery (arrow). (B) Proton-density image showing eccentric wall thickening and atherosclerotic plaques with a remodeling index of 1.47. (C) Contrast-enhanced T1-weighted image showing strong enhancement in eccentric atherosclerotic plaques.

http://dx.doi.org/10.5853/jos.2015.17.3.238

toms are present in 52% of patients with intracranial artery dissection, followed by subarachnoid hemorrhage in 28% of patients.[49] Intracranial artery dissection is estimated to be responsible for approximately 3%-5% of subarachnoid hemorrhage cases.[12] Intracranial artery dissection tends to be more common in Asian populations.[50] In European populations, intracranial artery dissection is believed to comprise < 10% of all spontaneous cervicocephalic artery dissections in adults,[51] but this percentage is > 90% in Asian populations.[49] This difference may also be associated with the higher incidence of intracranial atherosclerosis that is observed in Asian populations.

The conventional radiological findings of arterial dissection include intimal flap, double lumen, intramural hematoma, aneurysmal dilatation, tapered stenosis, and occlusion. The diagnostic criteria for intracranial artery dissection have been well organized by SASSY Japan (Strategies Against Stroke Study for Young Adults in Japan), which defines definite dissection and suspected dissection on luminal angiography. Definite cases include intimal flap and double lumen, and a clear geometric change on follow-up. Suspected cases include the string-of-pearls sign and tapered occlusion on luminal angiography, and intramural hematoma on conventional T1-weighted imaging.[52] However, these criteria may not apply to HR-MR12 because those were established mainly by using luminal angiography, including digital subtraction angiography.[49] The HR-MR findings of intracranial artery dissection are predominantly observed in the ver-

Table 1. Predominant HR-MRI characteristics of intracranial artery disease

	Atherosclerosis	Dissection	Moyamoya	Vasculitis	RCVS
Shape	Eccentric	Eccentric or combined	Concentric	Concentric (sometimes eccentric)	Concentric
Distribution	Any artery	Any artery (most common, VA)	Terminal ICA, proximal MCA, ACA	Medium- to small-sized vessels	Medium- to small-sized vessels
Signal intensity	Dependent on components (lipid, T1W iso/T2 hypo to iso; fibrous tissue, T1W/T2W iso; calcification, T1W/T2W dark)	Various (intramural hematoma, T1W hyper)			
Enhancement	Dependent on stage (+++ → +)	+/-	++/+	Dependent on stage (+++ → -)	Dependent on stage (+ → -)
Outer diameter	Positive or negative remodeling	Dependent on stage (Positive remodeling → restoration)	Negative remodeling		
Others	Intraplaque hemorrhage	Intimal flap, double lumen, intramural hematoma, or aneurysmal dilatation	Basal collaterals	Exclusive diagnosis	Exclusive diagnosis
Follow-up (resolution)	<30%	37.4%-75%	Progressive	Resolution with medication	Spontaneous reversibility

HR-MRI, high-resolution magnetic resonance imaging; RCVS, reversible cerebral vasoconstriction syndrome; VA, vertebral artery; ICA, internal carotid artery; MCA, middle cerebral artery; ACA, anterior cerebral artery.

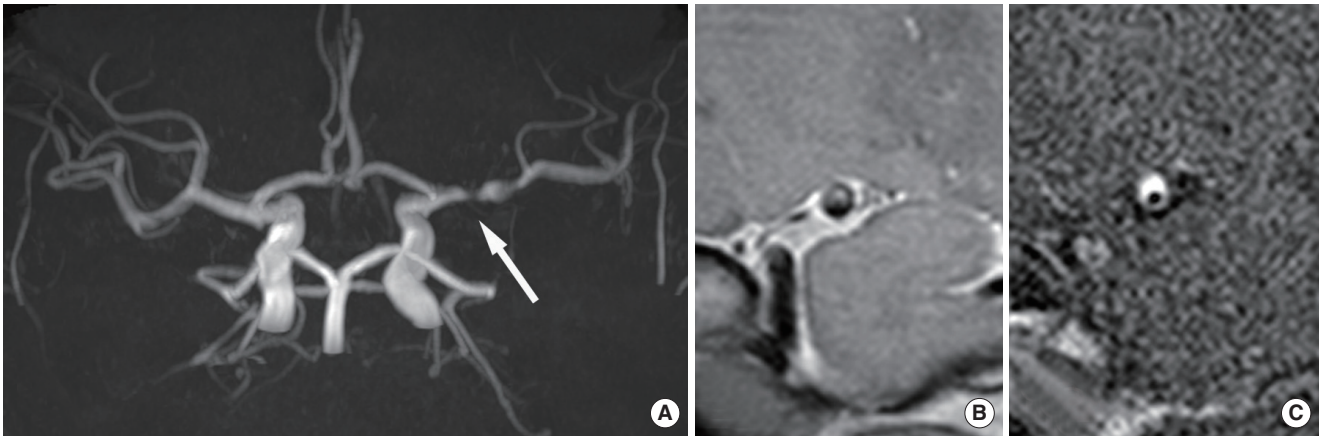

Figure 2. Intracranial atherosclerosis. A 58-year-old male patient presented with dizziness and three atherosclerotic risk factors. (A) Time-of-flight magnetic resonance angiograph showing severe stenosis in the left middle cerebral artery (arrow). (B) Proton-density image showing eccentric wall thickening and atherosclerotic plaques with a remodeling index of 1.04. (C) Contrast-enhanced T1-weighted image showing strong enhancement in eccentric atherosclerotic plaques.

tebral artery with the highest incidence (68.7%).[49] Wang et al. reported intramural hematoma in 61% of patients, double lumen in 50% of patients, and intimal flap in 42% of patients (in total, 76 patients with intracranial vertebral artery dissection were assessed[32]); however, intimal flap was the most common finding (91.4%) according to Han et al.[53] Recent reports indicate that intimal flap and double lumen are the most common findings seen on HR-MR in patients with middle cerebral artery dissection.[54,55] Vessel wall enhancement is sometimes associated with intracranial artery dissection. Although vessel wall enhancement is not completely understood, it has been considered to result from inflammation,[56] slow blood flow in the false lumen, or enhancement of the vasa vasorum.[57] A positron emission tomography (PET) study reported that vessel wall enhancement may indicate generalized transient inflammatory arteriopathy; in this study, the enhancement was resolved with vessel wall alteration in a matter of weeks.[56] In intracranial artery dissection, vessel wall enhancement may not be an uncommon finding.[57] Intramural hematoma is one of the most common findings on HR-MRI. If HR-MRI indicates intramural hematoma without intimal flap or double lumen, intracranial artery dissection should first be included as part of the differential diagnosis. However, the interpreter may have to consider the possibility of intraplaque hemorrhage in equivocal cases that also demonstrate the clinical features of atherosclerosis. In particular, the middle cerebral artery is one of the most common sites of intracranial atherosclerosis and may clinically present more often in equivocal cases. In addition, several pathological studies reported intramural hematoma with no connection between true and false lumen in intracranial vertebral-artery dissection, and which may have resulted from the rupture of the vasa vasorum or new vessels.[58] Therefore, the differentiation between intramural hematoma and intraplaque hemorrhage may sometimes be challenging and may depend on clinical information such as patient age, atherosclerotic risk factors, symptoms, and radiologic findings such as a clear geometric change seen on follow-up. Intramural hematoma can demonstrate various signal intensities, such as intraplaque hemorrhage. Although a bright high-signal intensity (73.9%) on T1-weighted imaging is the most common finding associated with intramural hematoma, isointensity (8.7%) and hypointensity (13%) can also be observed. On T2-weighted imaging, intramural hematoma can demonstrate hyperintensity (58.7%), isointensity (13%), or hypointensity (28.3%)[32] (Figure 3). Susceptibility-weighted imaging provides higher sensitivity for the detection of hemorrhage, a higher resolution than conventional T2-weighted gradient-echo imaging, and differentiation of hemorrhage from calcification with phase maps.[33] Recent studies suggested the usefulness of susceptibility-weighted imaging for the detection of intramural hematoma and the diagnosis of intracranial artery dissection.[54,59]

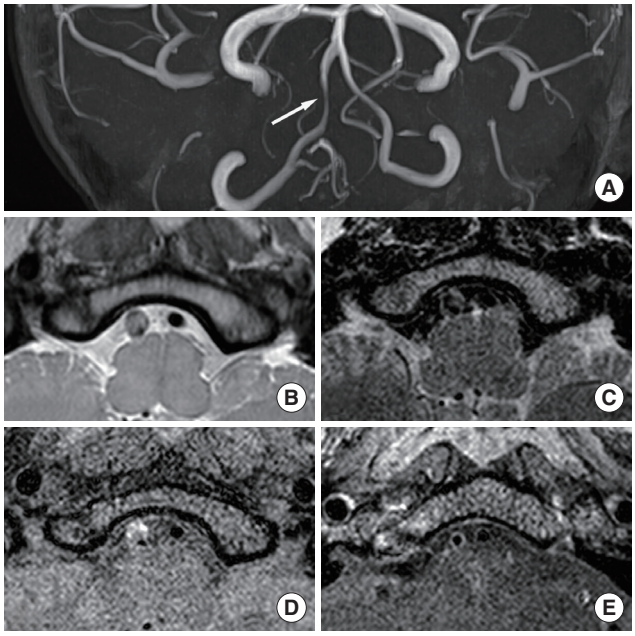

Figure 3. Intracranial artery dissection. A 37-year-old female patient presented with dizziness. (A) Time-of-flight magnetic resonance angiograph showing severe stenosis in the right vertebral artery (arrow). (B) Intramural hematoma and aneurysmal dilatation on proton-density imaging. (C) Intramural hematoma presenting as hyperintensity and hypointensity on T2-weighted imaging, and (D) intramural hematoma presenting as hyperintensity and isointensity on T1-weighted imaging. (E) Artery distal to the dissected segment showing periarterial enhancement on contrast-enhanced T1-weighted imaging.

Arterial dissection may be a dynamic vascular pathology, which explains why the diagnostic criteria include subsequent geometric change.[52] Intracranial artery dissection can be restored and result in complete normalization spontaneously.[60] Mizutani reported that 83.9% of unruptured intracranial artery dissections subsequently demonstrate geometric changes between 2 weeks and 2 months, and, among these, 61.5% demonstrate improvement in the dissecting lumen and 18.3% demonstrate complete normalization on serial follow-up angiography.[60] Of unruptured intracranial vertebral artery dissections, 37.4%-75% demonstrate improvement.[61,62] The resolution rate for intracranial artery dissection seems to be higher than that of intracranial atherosclerosis when intensive medication is administered (< 30%).[63,64] On HR-MRI, the cervical artery demonstrates intramural hematomas with hyperintensity at 2 weeks, and then the signal intensity decreases.[65] However, the natural course of these serial changes in intracranial artery dissection has been poorly studied. Therefore, HR-MR findings can change over time, and serial changes may have to be estimated to make a diagnosis and predict the prognosis (Figure 4).

With HR-MRI, intimal flap and double lumen can be defini-

http://dx.doi.org/10.5853/jos.2015.17.3.238

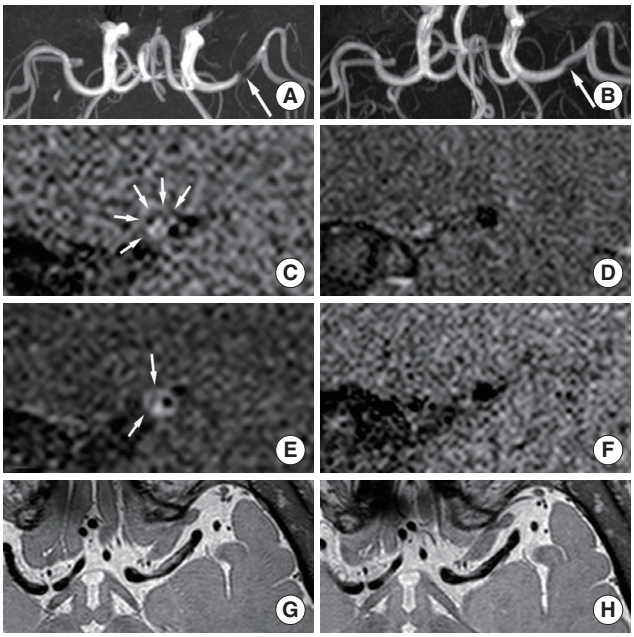

Figure 4. Intracranial artery dissection. A 50-year-old male patient with one atherosclerotic risk factor (smoking) presented with right-side weakness. (A) Time-of-flight magnetic resonance angiograph showing severe stenosis in the left middle cerebral artery (arrow). (C) Intramural hematoma showing hyperintensity on T1-weighted imaging (small arrows), and (E) the intimal flap seen on contrast-enhanced T1-weighted imaging (small arrows). (G) Segmental aneurysmal dilatation seen on proton-density imaging. (B) One year later, the dissecting lumen improved (arrow), and (D, F, H) the aforementioned findings disappeared. The patient was considered to have had a middle cerebral artery dissection; however, intraplaque hemorrhage underlying atherosclerosis could not be excluded completely.

tively diagnosed in intracranial artery dissections, and intramural hematoma and aneurysmal dilatation can be helpful criteria. However, these findings can also change on follow-up examinations (Table 1).

Moyamoya disease

Moyamoya disease is a cerebrovascular disease that is characterized by abnormal vascular networks, and spontaneous and progressive stenosis or occlusion at the terminus of the internal carotid artery. These abnormal vascular networks develop at the base of the brain and consist of collateral channels that compensate for ischemic changes in brain tissue.[66] Moyamoya disease is characterized by bilateral pathognomonic findings on angiography, whereas unilateral findings indicate moyamoya syndrome that will eventually progress into bilateral disease in up to 40% of patients.[67] Stenosis or occlusion occurs in the terminus of the internal carotid artery, and in the proximal anterior cerebral artery or middle cerebral artery. Intimal hyperplasia and medial thinning are well-known pathological characteristics. Intimal hyperplasia caused by the proliferation of smooth muscle cells and luminal thrombosis result in stenosis or occlusion. The media is thinned by the degradation and death of smooth muscle cells. Caspase-dependent apoptosis and overproduction of matrix metalloproteinase are considered contributory mechanisms.[68,69] Moyamoya disease demonstrates a natural course from stenosis in the terminal internal carotid artery with collateral networks to obliteration and the concomitant disappearance of collaterals,[66] thereby resulting in internal carotid to external carotid conversion.[69]

Distinguishing between moyamoya disease and atherosclerosis is sometimes difficult in East Asian populations, especially in patients with equivocal clinical and radiological findings (e.g., young patients with the typical angiographic pattern of moyamoya disease and atherosclerotic risk factors).[70] Moyamoya disease is primarily diagnosed on luminal angiography, such as digital subtraction angiography, according to pathognomonic findings. However, equivocal angiographic findings are sometimes seen in clinical settings. In equivocal cases, HR-MRI may help provide a more precise diagnosis and differentiation. A decrease in the outer diameter and concentric and weaker enhancement in the bilateral terminus of the internal cerebral artery, proximal anterior cerebral artery, or middle cerebral artery are characteristics of moyamoya disease that can be used to distinguish it from intracranial atherosclerosis.[11,71] Arterial wall degradation in association with media thinness may also contribute to decreasing the outer diameter in arterial segments. Intimal hyperplasia may indicate diffuse concentric enhancement.[11,71] The minimum outer diameter demonstrates a significant difference between conditions (1.61-2.01 mm for moyamoya disease vs. 3.03-3.31 mm for atherosclerosis[70,71]), and the remodeling index and wall area are significantly lower in moyamoya disease (mean remodeling index: 0.19 vs. 1.00; mean wall area: 0.32-0.39 vs. 1.64-6.00 mm^2 [11,70]). Concentric enhancement is higher in moyamoya disease,[11,71] but the degree of enhancement is lower[71] (Figures 5 and 6). Bilateral involvement is more common in moyamoya disease.[11] Although moyamoya disease is a representative vascular pathology presenting with decreasing outer diameter of vessels, interpreters may consider other conditions such as congenital agenesis, chronic state of localized arteritis, or dissection.[72,73] Nonenhanced T1-weighted and T2-weighted imaging also demonstrate a more homogeneous signal intensity. Depending on the progression of moyamoya disease, the outer diameter also significantly decreases. The radiological findings change over time, and typical moyamoya vessels are only seen during the intermediate stages, which may make it difficult to precisely diagnose this disorder[70] (Table 1).

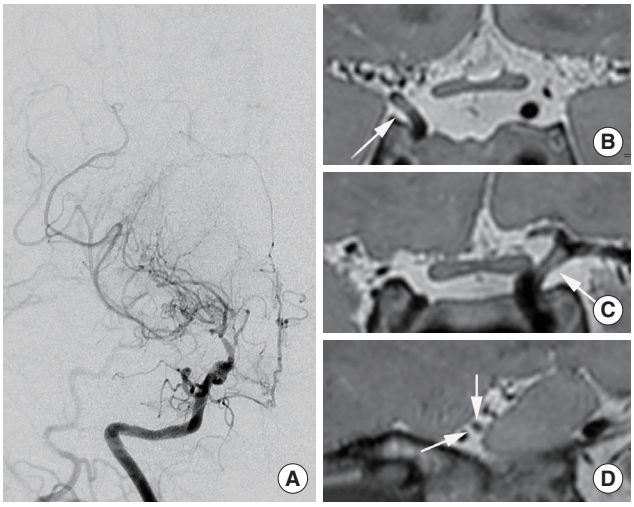

Figure 5. Moyamoya disease. A 50-year-old female patient presented with dizziness. (A) Digital subtraction angiography image showing severe stenosis in the right terminal internal carotid artery and middle cerebral artery with basal collaterals. (B, C) The outer diameters of both terminal internal carotid arteries (arrows) and (D) right middle cerebral artery (arrows) decreased (remodeling index, 0.18) on proton-density imaging.

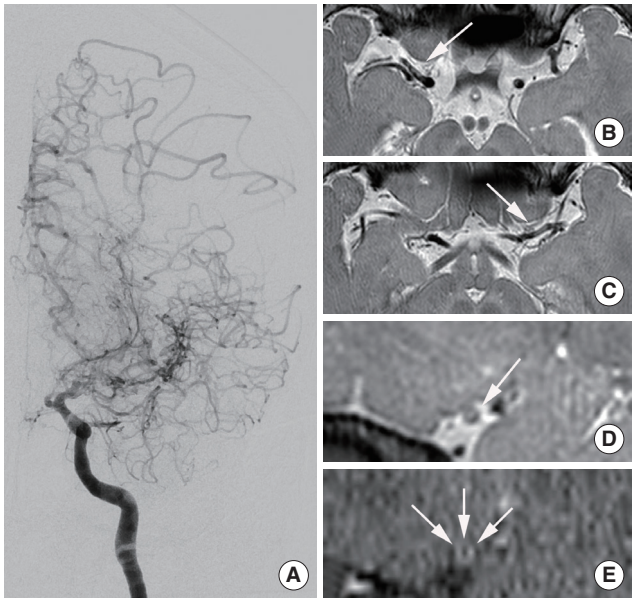

Figure 6. Moyamoya disease. A 44-year-old male patient presented with abulia. (A) Digital subtraction angiography image showing severe stenosis of the left terminal internal carotid artery and middle cerebral artery with basal collaterals. (B, C) The outer diameters of both middle cerebral arteries (arrows) decreased on proton-density imaging. (D) Left middle cerebral artery (arrow) showing a remodeling index of 0.31 on proton-density imaging with (E) concentric and mild enhancement (arrows) on contrast-enhanced T1-weighted imaging.

Vasculitis

Central nervous system (CNS) vasculitis encompasses a broad spectrum of cerebrovascular diseases that demonstrate various inflammatory and destructive characteristics. Its incidence is very rare, and the average annual rate is 2.4 cases per 1 million person-years.[74] Primary CNS vasculitis refers to primary angiitis in the CNS, and secondary CNS vasculitis develops as a result of systemic inflammatory or infectious conditions.[75] Primary angiitis in the CNS was diagnosed in the exclusive work by Calabrese and Mallek who proposed the following criteria: (i) an acquired or otherwise unexplainable neurological or psychiatric deficit, (ii) classic features of angiitis on angiographic or histopathological study, and (iii) no evidence of secondary vasculitis.[76] The major differential diagnoses are intracranial atherosclerosis or RCVS. Intracranial atherosclerosis can be excluded according to atherosclerotic risk factors, normal cerebrospinal fluid findings,[75] and classic angiographic and HR-MR findings. RCVS can also be differentiated by using the clinical and HR-MR findings, as mentioned below. The HR-MR characteristics of intracranial atherosclerosis may include eccentric and irregular atherosclerotic plaques that predominantly develop in the more proximal intracranial arteries (e.g., distal internal carotid artery and proximal cerebral arteries), whereas smooth wall thickening is usually noted in medium- to small-sized arteries during vasculitis. The medium-sized arteries mean distal to the bifurcation of the middle cerebral artery and the anterior and posterior communicating arteries. Small-sized arteries are beyond the resolution of digital subtraction angiography.[77,78] Vasculitis can also show smooth concentric or eccentric wall thickening and enhancement.[77] The degree of enhancement indicates the activity of vasculitis. Therefore, favorable treatment responses can decrease the degree of enhancement.[79,80] Arterial involvement is more common in single lesions that develop in multiple arteries than multiple lesions that develop in a single artery.[78] In the case of multiple ischemic strokes with different ages in different vascular territories, vasculitis can be suspected[75] (Table 1).

RCVS

RCVS is also called benign cerebral vasculitis because it demonstrates clinical characteristics and radiological findings similar to those of vasculitis; however, RCVS also demonstrates a benign prognosis with complete normalization.[81,82] The suggested diagnostic criteria for RCVS include the following: (i) headache with sudden thunderclap, and severe recurrent features with or without additional neurologic signs or symptoms; (ii) normal or near-normal cerebrospinal fluid; (iii) no evidence of aneurysmal subarachnoid hemorrhage; (iv) alternating constriction, normal vascular caliber, or dilatation on angiography; and (v) the spontaneous complete or near-complete reversal of vasoconstriction within 3 months.[83,84] The most specific criterion is reversibility.[83] HR-MRI can differentiate RCVS from CNS vasculitis according

http://dx.doi.org/10.5853/jos.2015.17.3.238

to the following features: less, diffuse, uniform, and continuous wall thickening and enhancement; a shorter interval to restore (3 months vs. 7-17 months); and a higher rate of resolution (88.9% vs. 33.3%), in comparison with vasculitis.[77,84] Although the pathophysiology remains unclear, alterations in cerebral vascular tone are associated with various exogenous and endogenous factors that are believed to cause RCVS.[83] The shortening and overlapping of smooth muscle cells result in increased wall thickness and luminal stenosis according to an experimental vasospasm study, which may explain the wall thickening observed on HR-MR.[85] The absence of arterial inflammation in RCVS may be consistent with weak enhancement on HR-MR[81,82] (Table 1).

Vessel wall imaging of cervical carotid artery atherosclerosis

About 15%-30% of all ischemic strokes were associated with cervical carotid atherosclerosis.[86,87] Significant cervical carotid artery stenosis (> 50% on carotid US) has a prevalence of 7%-10%; it is predominantly caused by atherosclerosis,[88] and its prevalence increases in populations with high atherosclerotic risk factors, cardiac disease, or acute stroke.[89] The degree of carotid artery stenosis is considered the parameter of choice for determining the best therapeutic approach. The correlation between the severity of carotid stenosis and the risk of cardiovascular events has been widely reported.[90,91] The most widely used methods for measuring the degree of stenosis include the North American Symptomatic Carotid Endarterectomy Trial (NASCET) and the European Carotid Surgery Trial (ECST), both of which evaluate the degree of stenosis as the percentage reduction in the linear diameter of the carotid artery. The NASCET method calculates the ratio between the luminal diameter at the stenotic area and the luminal diameter of the distal, healthy carotid artery. The ECST method calculates the ratio between the luminal diameter at the stenotic area and the total carotid artery diameter (including the plaque). However, there is a difference between methods (e.g., 70% on NASCET usually corresponds to 83% on ECST), and this difference cannot be overcome, even if the NASCET and ECST measurements are converted to each other.[92] Previous studies report that the methods of percentage stenosis measurement are also susceptible to interobserver variability and errors, mostly owing to the incorrect identification of the arterial reference points.[10,92] Several recent studies show that moderate carotid artery stenosis may lead to cardiovascular events, and subsequent histopathologic studies demonstrate that plaque erosion and disruption are common morphologic features in symptomatic lesions, thereby indicating that luminal narrowing is not the sole predictor of stroke.[93-95] Because low-grade carotid artery stenosis (< 30%) can produce cerebrovascular events, several factors are considered important biomarkers for predicting future stroke,[96] including carotid plaque composition, the presence and state of the fibrous cap, plaque hemorrhage, plaque ulceration, and plaque location.[97] Therefore, the concept of "vulnerable plaques" was introduced to the surgical, histopathological, and imaging communities, which refers to atheromas that contain a thin fibrous cap with a large, lipid-rich, necrotic core, intraplaque hemorrhage, and the presence of active intraplaque inflammation, thereby making it more prone to rupture, embolization, and thrombosis.[10]

In subsequent sections, we will detail the roles of various vessel wall imaging techniques for assessing cervical carotid artery pathology, with a specific emphasis on plaque morphology and characteristics.

Vessel wall imaging techniques

US

US with color Doppler is globally accepted as the first-line imaging modality for diagnosing atherosclerotic cervical carotid artery disease, the degree of stenosis with blood-flow velocity profiles, the shape and type of plaque, and the intima-media thickness (IMT). This noninvasive, high-resolution imaging technique is readily available and inexpensive. High-frequency linear transducers (> 7 MHz) are ideal for measuring carotid wall thickness, as well as for qualitatively and quantitatively analyzing plaques. Moreover, low-frequency linear transducers (< 7 MHz) are preferred for Doppler examinations.[10] US with color Doppler is a good screening technique; however, several limitations persist when using this method to quantify the degree of stenosis, including reproducibility, artifacts due to calcifications, and difficulty in differentiating between subtotal and total occlusion.[98,99] It is well known that Doppler velocity increases in proportion to the degree of stenosis, and therefore flow velocity is commonly used to evaluate the severity of carotid stenosis. Several studies report different peak systolic velocities (220-283 cm/s), which correlate with 70% on the NASCET[100-102] (Table 2). In terms of plaque shape, surface irregularities also demonstrate markers of plaque vulnerability and are predictive of ischemic stroke (Figure 7).[103,104] Echolucent plaques are also associated with higher concentrations of soft-tissue components, such as fibrofatty and hemorrhagic contents (i.e., vulnerable plaques). Several studies report asymptomatic patients with echolucent plaques as being at high risk for ischemic stroke[105,106] (Figure 8). Nevertheless, there are conflicting studies on echogenicity, and there is no association between ischemic stroke and echolucent plaques.[107] This could be explained by the poor reproducibility of the sub-

Table 2. Gray-scale and Doppler US criteria for diagnosing ICA stenosis

Degree of stenosis (%)	Primary parameters		Additional parameters	
	ICA PSV (cm/s)	Plaque estimate (%)	ICA/CCA PSV ratio	ICA EDV (cm/s)
Normal	<125	None	<2.0	<40
<50	<125	<50	<2.0	<40
50-69	125-230	≥50	2.0-4.0	40-100
≥70 but less than near occlusion	>230	≥50	>4.0	>100
Near occlusion	High, low, or undetectable	Visible	Variable	Variable
Total occlusion	Undetectable	Visible, no detectable lumen	Not applicable	Not applicable

US, ultrasound; ICA, internal carotid artery; PSV, peak systolic velocity; CCA, common carotid artery; EDV, end diastolic velocity.

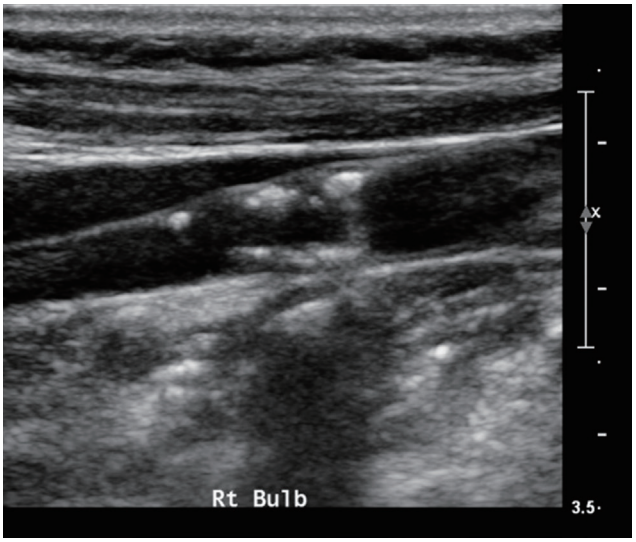

Figure 7. Ultrasound (US) example of an irregular plaque. The US image shows a large amount of irregular-appearing heterogeneous plaque with multifocal calcification (bright areas with shadowing) in the carotid artery.

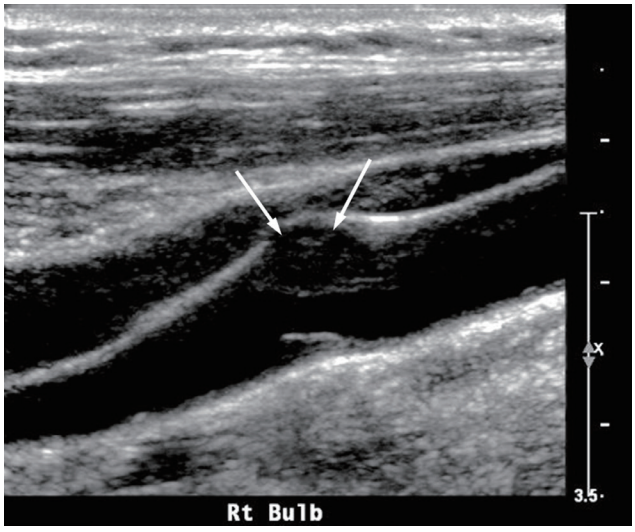

Figure 8. Ultrasound (US) example of an echolucent plaque. The US image shows a smooth echolucent plaque (arrows) on the carotid wall.

jective characterization of plaque echogenicity by using B-mode US; however, this remains an ongoing subject of research.[59]

US with color Doppler can also assess IMT, and an increase in the IMT of the common carotid artery could be used to predict cardiovascular events.[103,108] The arterial wall may demonstrate two parallel echogenic lines that are separated by a relatively hypoechoic intermediate area on longitudinal B-mode US, and the distance between these lines is the IMT (Figure 9). Carotid IMT could also be measured by using an automated imaging processing software.

CT

With the introduction of multidetector CT and advanced software for image reconstruction, this method provides improved spatial and temporal resolution and is a reliable tool for evaluating cervical carotid arterial pathology. With CT angiography, investigators can evaluate not only carotid stenosis but also the morphology of carotid plaques. A meta-analysis of the diagnostic accuracy of CT angiography for assessing carotid artery stenosis, in comparison with that of CT angiography and digital subtraction angiography, reports that CT angiography is

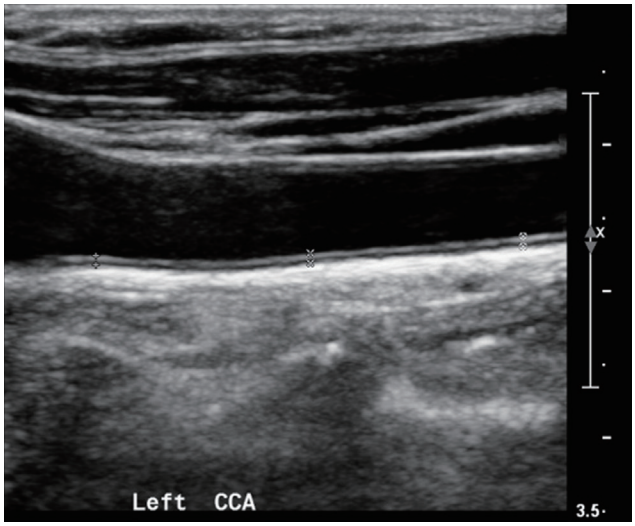

Figure 9. Normal carotid artery showing sites for measuring intima-media thickness. The arterial wall may demonstrate two parallel echogenic lines that are separated by a relatively hypoechoic intermediate area on longitudinal ultrasound, and the distance between these lines is the intima-media thickness.

http://dx.doi.org/10.5853/jos.2015.17.3.238

reliably accurate for diagnosing severe stenosis (>70%) (85% sensitivity and 93% specificity). CT angiography is also highly accurate when diagnosing the degree of carotid occlusion (97% sensitivity and 99% specificity).[109] In terms of plaque morphology, the most relevant surface alteration that may be detected on CT angiography is ulceration (Figure 10).[10] Saba et al. reported that CT angiography has a significantly higher diagnostic accuracy for plaque ulceration than US (93% vs. 37.5%, respectively) (the presence of ulceration in surgery was used as the gold standard).[110] Several studies that used CT angiography differentiated carotid artery plaques into three categories (fatty, mixed, and calcified lesions), according to the criteria reported by Schroeder et al.[111]: fatty plaques demonstrate an attenuation of <50 HU; mixed plaques demonstrate an attenuation of between 50 and 119 HU; and calcified plaques demonstrate an attenuation of >120 HU (Figure 11). There is also a moderate correlation between HU measurement and histopathology, and CT demonstrates good accuracy when detecting calcification. However, CT angiography demonstrates a lower accuracy when differentiating other components (e.g., lipid core and hemorrhage) in comparison with MRI.[10,110,112] The other drawbacks of CT angiography include radiation, potential intolerable contrast agents, and contrast-induced nephropathy.

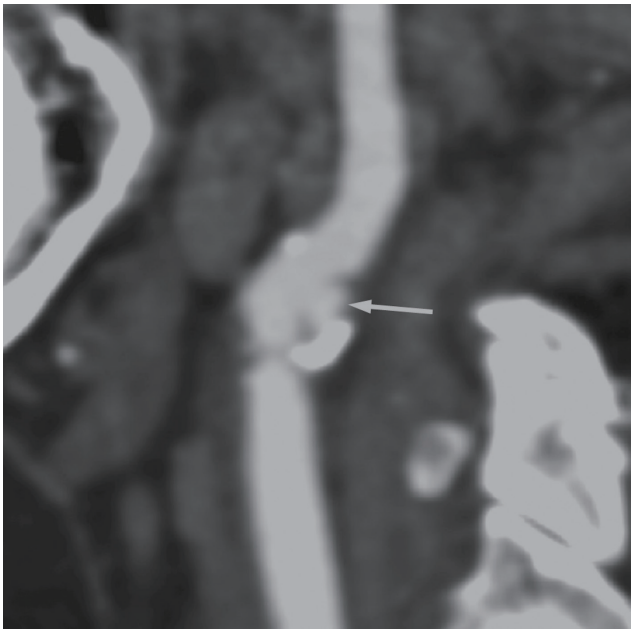

Figure 10. Computed tomography angiographic image showing ulcerated plaque (arrows) with calcification in the carotid artery.

HR-MRI

Recent developments in receiver coil and pulse sequence design potentially allow using HR-MRI to assess carotid plaques.[6,113,114] MRI provides information about (i) the degree of stenosis, (ii) total plaque volume, (iii) plaque components, and (iv) plaque surface morphology, including ulceration and fibrous cap rupture.[115-117] This identification allows serial monitoring of carotid plaque evolution and the identification of the risk factors for accelerated progression.[116,118]

The combination of multiple MR pulse sequences such as T1- and T2-weighted, proton-density, and time-of-flight (TOF) imaging, by containing black- and bright-blood sequences, is needed to characterize plaque morphology and its components.[119] The MR signal intensities of the carotid plaque components, including the lipid core, hemorrhage, calcification, and fibrous tissues, are described in Table 3 and Figure 12.

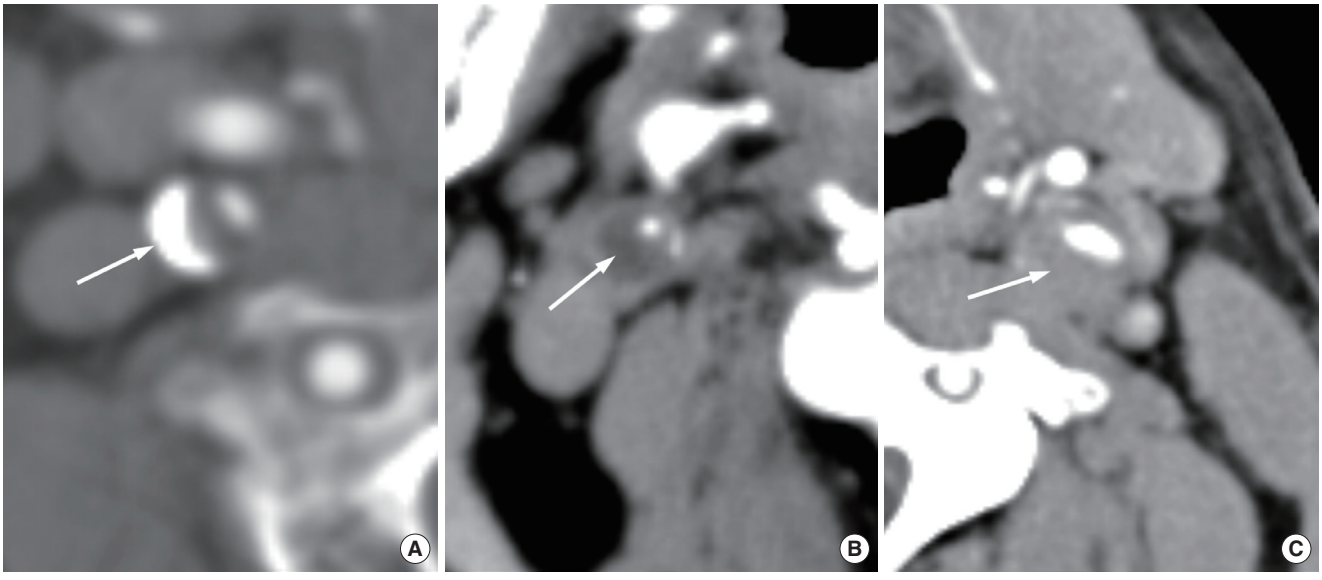

Figure 11. Different carotid plaques on computed tomography angiography. Arrow indicates (A) calcified, (B) fatty, and (C) mixed plaque.

Table 3. Signal intensity of the carotid plaque components on MRI

Plaque component	3D TOF image	T1-weighted image	T2-weighted image	Proton density image	Contrast-enhanced T1-weighted image
Lipid core	Iso	Iso/hyper	Hypo	Iso/hyper	-
Fibrous tissue	Iso	Iso/hyper	Iso/hyper	Iso/hyper	+
Hemorrhage					
Fresh (<1 week)	Hyper	Hyper	Iso/hypo	Iso/hypo	-
Recent (1-6 weeks)	Hyper	Hyper	Hyper	Hyper	-
Chronic (>6 weeks)	Hypo	Hypo	Hypo	Hypo	-
Calcification	Marked hypo	Marked hypo	Marked hypo	Marked hypo	-

MRI, magnetic resonance imaging; 3D TOF, three-dimensional time of flight.

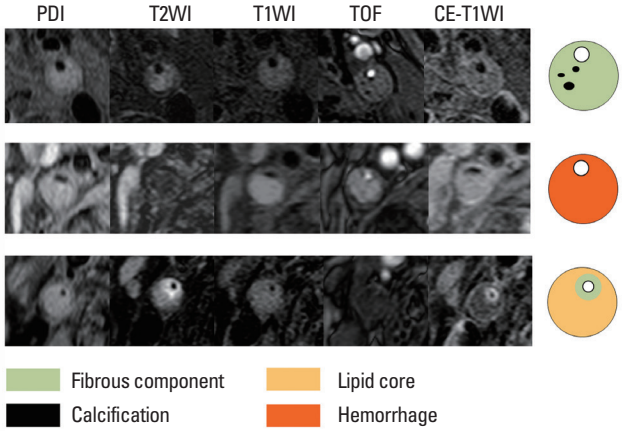

Figure 12. Four main components of atherosclerotic plaques. Axial magnetic resonance images obtained by using five pulse sequences. The fibrous component is isointense on T1WI, T2WI, and PDI with enhancement. Fresh hemorrhage is hyperintense on T1WI and TOF imaging and hypointense on T2WI without enhancement. The lipid core is the area that demonstrates a drop in signal intensity from PDI to T2WI. The calcification demonstrates dark signal intensity on all sequences.

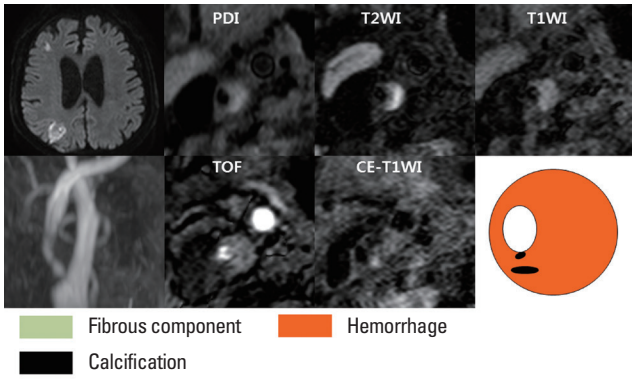

Figure 13. Vulnerable plaque. Axial diffusion-weighted magnetic resonance (MR) image of the brain (top right) and MR angiographic image (bottom right) showing high-grade carotid stenosis with ipsilateral acute infarction. Axial MR images obtained by using five pulse sequences show that the plaque contains three components. A large recent hemorrhage is hyperintense on T1- and T2-weighted imaging, proton-density imaging, and TOF imaging, and multifocal calcifications are hypointense in all sequences. PDI, proton density image; T2WI, T2-weighted image; T1WI, T1-weighted image; TOF, time-of-flight image; CE-T1WI, contrast enhanced T1-weighted image.

According to previous studies, the signal intensities of the lipid cores vary on T2-weighted imaging.[120,121] These variations in signal intensity seem to result from (i) the different entities of the lipid cores (liquid vs. solid) and (ii) differences in the echo times used on T2-weighted imaging.[122] Two-thirds of the lipids in the lipid core are in the solid or semiliquid phase, which demonstrate very poor signals; moreover, it is difficult to directly image the lipidic components.[123] Some of the lipids in the plaque tend to liquify at body temperature, which may demonstrate higher signal intensities on T2-weighted imaging. The lipid cores in the liquid phase may flow out through a fissure or ruptured site of the fibrous cap in the carotid lumen, thereby resulting in cerebrovascular embolism. In contrast, organized lipid cores are firmer, more stable, and resistant to mechanical pressure.[122,124] With multiple MR sequencing, previous studies report higher sensitivities (87%) and specificities (92%) when identifying lipid cores.[119] The lipid core is isointense on proton-density imaging, and the intensity decreases on T2-weighted imaging (i.e., the signal intensity is lower on T2-weighted imaging than in proton-density imaging); moreover, it shows lesser enhancement than do fibrous tissues on contrast-enhanced T1-weighted imaging.[115]

Intraplaque hemorrhage is the critical step in the progression and destabilization of atherosclerotic plaques in the carotid artery.[125] The signal intensity of intraplaque hemorrhage depends on its oxidative state and the structure of hemoglobin. Fresh hemorrhage (<1 week) corresponds to intracellular methemoglobin (early subacute cerebral hemorrhage) and is hyperintense on T1-weighted and TOF images, but isointense or hypointense on T2-weighted and proton-density images. Recent intraplaque hemorrhage (1-6 weeks), which corresponds to extracellular methemoglobin (late subacute stage cerebral hemorrhage), is hyperintense on all four sequences. Chronic hemorrhage (>6 weeks) corresponds to extracellular hemosiderin and is hypointense on all four sequences[117,118] (Figure 13).

The fibrous component corresponds to the extracellular matrix, which modifies the water-protein interactions and is isointense or moderately hyperintense relative to the adjacent muscles on T1-weighted, T2-weighted, and proton-density images,

http://dx.doi.org/10.5853/jos.2015.17.3.238

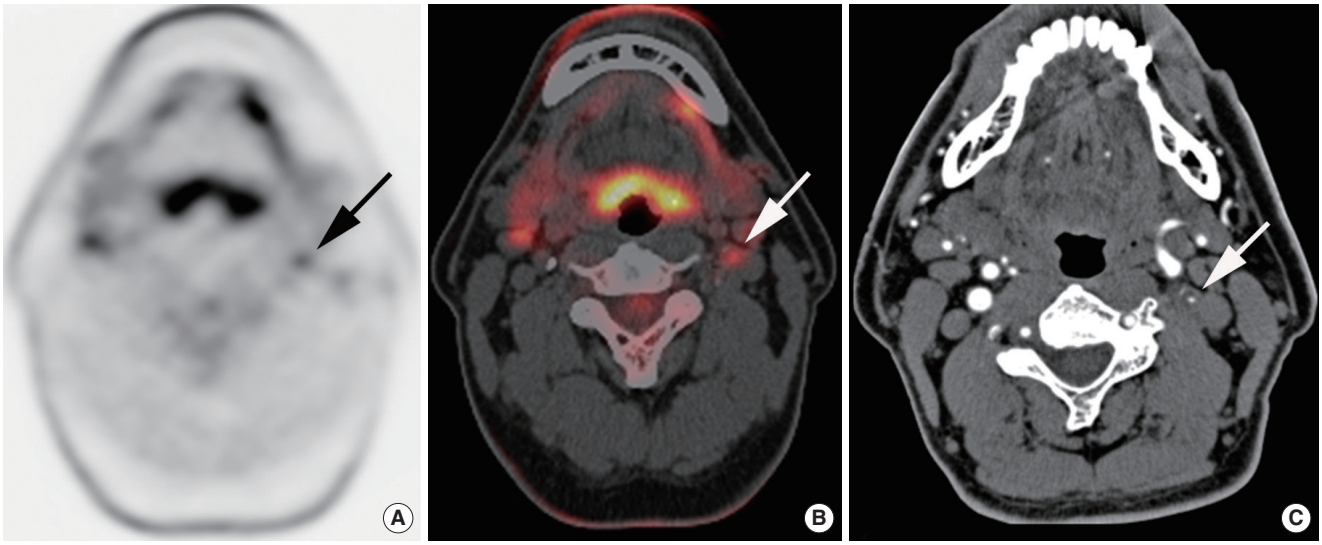

Figure 14. Positron emission tomography-computed tomography (PET-CT): arrow indicates (A) ^{18}F-FDG PET and (B) PET-CT showing a high uptake in left internal carotid artery, and (C) CT angiography showing severe stenosis of the left internal carotid artery with an atherosclerotic plaque.

but isointense on TOF MRI. On contrast-enhanced T1-weighted images, fibrous tissue demonstrates enhancement but lipid-rich necrotic cores do not show enhancement.[126] Calcifications consist of calcium hydroxyapatite. MRI shows calcifications as markedly hypointense areas on all four sequences.

To identify these components in carotid plaques, the following reading scheme is proposed[6,127]: (i) define calcified areas (hypointense on all four sequences); (ii) define recent or fresh hemorrhage (hyperintense on T1-weighted and TOF MRI); (iii) define the lipid core (focal decrease in signal intensity from proton-density to T2-weighted imaging) in areas without calcifications or hemorrhage; and (iv) assign a fibrous component to the remaining areas. Plaque inflammation is a recognized risk factor for plaque vulnerability. There is also a correlation between the degree of enhancement after administering gadolinium-based contrast media and plaque inflammation.[6] To improve the detection of plaque inflammation, several targeted MRI agents, including ultra-small superparamagnetic iron oxide particles, have been developed. Howarth et al.[128] reported that the uptake of ultra-small superparamagnetic iron oxide particles is more frequently observed in the carotid plaques of symptomatic patients than asymptomatic patients.

PET-CT

Several studies recently assessed the diagnostic potential of using ^{18}F-fluorodeoxyglucose PET (^{18}F-FDG PET) or ^{18}F-FDG PET/CT to evaluate plaque inflammation, and promising results have been reported. These studies report that ^{18}F-FDG PET or ^{18}F-FDG PET/CT can accurately detect high-risk carotid plaques[129-131] (Figure 14). There are significant correlations between the histologic findings and degree of inflammation on ^{18}F-FDG.[132,133] However, there are some fundamental limitations to using PET, including poor spatial limitation, susceptibility to partial volume effects, lack of quantification, and absence of standardized imaging protocols.[129] Further studies are needed to further clarify the role of FDG-PET in atherosclerosis imaging.

Conclusion

The etiology of ischemic stroke caused by intracranial and carotid artery disease is important when determining treatment options and predicting prognosis. Vessel wall imaging can be an adjunctive or alternative diagnostic method to traditional luminal angiography for depicting vascular pathology. In the intracranial artery, HR-MRI may provide a more precise etiology by taking into account signal intensity, enhancement, shape, numerical survey results (e.g., diameter, area, and length), and the location of the vascular walls. Currently, HR-MRI still presents substantial equivocal and overlapping findings for various intracranial vascular pathologies. Therefore, HR-MR results, clinical characteristics, and laboratory findings can provide a clear diagnosis and etiology. With the development of additional technologies and further studies, HR-MR will most likely play an important role in evaluating intracranial artery disease.

Characterizing the components of atherosclerotic plaques in the cervical carotid artery is a fundamental step to determining the optimal therapy. Improving the imaging techniques would allow the further study of vulnerable plaques, and increasing precision would allow patients to be stratified according to risk. Vessel wall imaging by using CT, MR, and US with color Doppler is

a useful and reliable method; however, the applications of nuclear medicine are still confined to clinical research.

References

1. Kernan WN, Ovbiagele B, Black HR, Bravata DM, Chimowitz MI, Ezekowitz MD, et al. Guidelines for the prevention of stroke in patients with stroke and transient ischemic attack: a guideline for healthcare professionals from the American Heart Association/American Stroke Association. *Stroke* 2014;45:2160-2236.
2. Hong KS, Bang OY, Kang DW, Yu KH, Bae HJ, Lee JS, et al. Stroke statistics in Korea: part I. Epidemiology and risk factors: a report from the Korean Stroke Society and Clinical Research Center for Stroke. *J Stroke* 2013;15:2-20.
3. Johnston SC, Mendis S, Mathers CD. Global variation in stroke burden and mortality: estimates from monitoring, surveillance, and modelling. *Lancet Neurol* 2009;8:345-354.
4. Dieleman N, van der Kolk AG, Zwanenburg JJ, Harteveld AA, Biessels GJ, Luijten PR, et al. Imaging intracranial vessel wall pathology with magnetic resonance imaging: current prospects and future directions. *Circulation* 2014;130:192-201.
5. Ryu CW, Kwak HS, Jahng GH, Lee HN. High-resolution MRI of intracranial atherosclerotic disease. *Neurointervention* 2014;9:9-20.
6. Oppenheim C, Naggara O, Touze E, Lacour JC, Schmitt E, Bonneville F, et al. High-resolution MR imaging of the cervical arterial wall: what the radiologist needs to know. *Radiographics* 2009;29:1413-1431.
7. Hur J, Park J, Kim YJ, Lee HJ, Shim HS, Choe KO, et al. Use of contrast enhancement and high-resolution 3D black-blood MRI to identify inflammation in atherosclerosis. *JACC Cardiovasc Imaging* 2010;3:1127-1135.
8. Wang J, Yarnykh VL, Hatsukami T, Chu B, Balu N, Yuan C. Improved suppression of plaque-mimicking artifacts in black-blood carotid atherosclerosis imaging using a multislice motion-sensitized driven-equilibrium (MSDE) turbo spin-echo (TSE) sequence. *Magn Reson Med* 2007;58:973-981.
9. Zhu C, Graves MJ, Yuan J, Sadat U, Gillard JH, Patterson AJ. Optimization of improved motion-sensitized driven-equilibrium (iMSDE) blood suppression for carotid artery wall imaging. *J Cardiovasc Magn Reson* 2014;16:61.
10. Saba L, Anzidei M, Sanfilippo R, Montisci R, Lucatelli P, Catalano C, et al. Imaging of the carotid artery. *Atherosclerosis* 2012;220:294-309.
11. Ryoo S, Cha J, Kim SJ, Choi JW, Ki CS, Kim KH, et al. High-resolution magnetic resonance wall imaging findings of Moyamoya disease. *Stroke* 2014;45:2457-2460.
12. Sikkema T, Uyttenboogaart M, Eshghi O, De Keyser J, Brouns R, van Dijk JM, et al. Intracranial artery dissection. *Eur J Neurol* 2014;21:820-826.
13. Sacco RL, Kargman DE, Zamanillo MC. Race-ethnic differences in stroke risk factors among hospitalized patients with cerebral infarction: the Northern Manhattan Stroke Study. *Neurology* 1995;45:659-663.
14. Sacco RL, Kargman DE, Gu Q, Zamanillo MC. Race-ethnicity and determinants of intracranial atherosclerotic cerebral infarction. The Northern Manhattan Stroke Study. *Stroke* 1995;26:14-20.
15. Wong LK. Global burden of intracranial atherosclerosis. *Int J Stroke* 2006;1:158-159.
16. Gorelick PB, Wong KS, Bae HJ, Pandey DK. Large artery intracranial occlusive disease: a large worldwide burden but a relatively neglected frontier. *Stroke* 2008;39:2396-2399.
17. White H, Boden-Albala B, Wang C, Elkind MS, Rundek T, Wright CB, et al. Ischemic stroke subtype incidence among whites, blacks, and Hispanics: the Northern Manhattan Study. *Circulation* 2005;111:1327-1331.
18. Makowski MR, Botnar RM. MR imaging of the arterial vessel wall: molecular imaging from bench to bedside. *Radiology* 2013;269:34-51.
19. Singh N, Moody AR, Gladstone DJ, Leung G, Ravikumar R, Zhan J, et al. Moderate carotid artery stenosis: MR imaging-depicted intraplaque hemorrhage predicts risk of cerebrovascular ischemic events in asymptomatic men. *Radiology* 2009;252:502-508.
20. Chu B, Ferguson MS, Chen H, Hippe DS, Kerwin WS, Canton G, et al. Magnetic resonance imaging features of the disruption-prone and the disrupted carotid plaque. *JACC Cardiovasc Imaging* 2009;2:883-896.
21. Fleg JL, Stone GW, Fayad ZA, Granada JF, Hatsukami TS, Kolodgie FD, et al. Detection of high-risk atherosclerotic plaque: report of the NHLBI Working Group on current status and future directions. *JACC Cardiovasc Imaging* 2012;5:941-955.
22. Jain KK. Some observations on the anatomy of the middle cerebral artery. *Can J Surg* 1964;7:134-139.
23. Kamath S. Observations on the length and diameter of vessels forming the circle of Willis. *J Anat* 1981;133:419-423.
24. Qiao Y, Zeiler SR, Mirbagheri S, Leigh R, Urrutia V, Wityk R, et al. Intracranial plaque enhancement in patients with cerebrovascular events on high-spatial-resolution MR images. *Radiology* 2014;271:534-542.
25. Chen XY, Wong KS, Lam WW, Ng HK. High signal on T1 sequence of magnetic resonance imaging confirmed to be intraplaque haemorrhage by histology in middle cerebral artery. *Int J Stroke* 2014;9:E19.

http://dx.doi.org/10.5853/jos.2015.17.3.238

26. Meyers PM, Schumacher HC, Gray WA, Fifi J, Gaudet JG, Heyer EJ, et al. Intravascular ultrasound of symptomatic intracranial stenosis demonstrates atherosclerotic plaque with intraplaque hemorrhage: a case report. *J Neuroimaging* 2009;19:266-270.
27. Xu WH, Li ML, Gao S, Ni J, Yao M, Zhou LX, et al. Middle cerebral artery intraplaque hemorrhage: prevalence and clinical relevance. *Ann Neurol* 2012;71:195-198.
28. Caruso RD, Postel GC, McDonald CS, Sherry RG. High signal on T1-weighted MR images of the head: a pictorial essay. *Clin Imaging* 2001;25:312-319.
29. Altaf N, MacSweeney ST, Gladman J, Auer DP. Carotid intraplaque hemorrhage predicts recurrent symptoms in patients with high-grade carotid stenosis. *Stroke* 2007;38:1633-1635.
30. Turan TN, Bonilha L, Morgan PS, Adams RJ, Chimowitz MI. Intraplaque hemorrhage in symptomatic intracranial atherosclerotic disease. *J Neuroimaging* 2011;21:e159-161.
31. Saito A, Sasaki M, Ogasawara K, Kobayashi M, Hitomi J, Narumi S, et al. Carotid plaque signal differences among four kinds of T1-weighted magnetic resonance imaging techniques: a histopathological correlation study. *Neuroradiology* 2012;54:1187-1194.
32. Wang Y, Lou X, Li Y, Sui B, Sun S, Li C, et al. Imaging investigation of intracranial arterial dissecting aneurysms by using 3 T high-resolution MRI and DSA: from the interventional neuroradiologists' view. *Acta Neurochir (Wien)* 2014;156:515-525.
33. Kim TW, Choi HS, Koo J, Jung SL, Ahn KJ, Kim BS, et al. Intramural hematoma detection by susceptibility-weighted imaging in intracranial vertebral artery dissection. *Cerebrovasc Dis* 2013;36:292-298.
34. Chen XY, Wong KS, Lam WW, Zhao HL, Ng HK. Middle cerebral artery atherosclerosis: histological comparison between plaques associated with and not associated with infarct in a postmortem study. *Cerebrovasc Dis* 2008;25:74-80.
35. Turan TN, Rumboldt Z, Granholm AC, Columbo L, Welsh CT, Lopes-Virella MF, et al. Intracranial atherosclerosis: correlation between in-vivo 3T high resolution MRI and pathology. *Atherosclerosis* 2014;237:460-463.
36. Mineyko A, Kirton A, Ng D, Wei XC. Normal intracranial perivascular enhancement on pediatric brain MR imaging. *Neuroradiology* 2013;55:1161-1169.
37. Skarpathiotakis M, Mandell DM, Swartz RH, Tomlinson G, Mikulis DJ. Intracranial atherosclerotic plaque enhancement in patients with ischemic stroke. *AJNR Am J Neuroradiol* 2013;34:299-304.
38. Vakil P, Vranic J, Hurley MC, Bernstein RA, Korutz AW, Habib A, et al. T1 gadolinium enhancement of intracranial atherosclerotic plaques associated with symptomatic ischemic presentations. *AJNR Am J Neuroradiol* 2013;34:2252-2258.
39. Sluimer JC, Kolodgie FD, Bijnens AP, Maxfield K, Pacheco E, Kutys B, et al. Thin-walled microvessels in human coronary atherosclerotic plaques show incomplete endothelial junctions relevance of compromised structural integrity for intraplaque microvascular leakage. *J Am Coll Cardiol* 2009;53:1517-1527.
40. Qiao Y, Etesami M, Astor BC, Zeiler SR, Trout HH 3rd, Wasserman BA. Carotid plaque neovascularization and hemorrhage detected by MR imaging are associated with recent cerebrovascular ischemic events. *AJNR Am J Neuroradiol* 2012;33:755-760.
41. Xu WH, Li ML, Gao S, Ni J, Zhou LX, Yao M, et al. Plaque distribution of stenotic middle cerebral artery and its clinical relevance. *Stroke* 2011;42:2957-2959.
42. Swartz RH, Bhuta SS, Farb RI, Agid R, Willinsky RA, Terbrugge KG, et al. Intracranial arterial wall imaging using high-resolution 3-tesla contrast-enhanced MRI. *Neurology* 2009;72:627-634.
43. Yamagishi M, Terashima M, Awano K, Kijima M, Nakatani S, Daikoku S, et al. Morphology of vulnerable coronary plaque: insights from follow-up of patients examined by intravascular ultrasound before an acute coronary syndrome. *J Am Coll Cardiol* 2000;35:106-111.
44. Zhu XJ, Du B, Lou X, Hui FK, Ma L, Zheng BW, et al. Morphologic characteristics of atherosclerotic middle cerebral arteries on 3T high-resolution MRI. *AJNR Am J Neuroradiol* 2013;34:1717-1722.
45. Chung GH, Kwak HS, Hwang SB, Jin GY. High resolution MR imaging in patients with symptomatic middle cerebral artery stenosis. *Eur J Radiol* 2012;81:4069-4074.
46. Xu WH, Li ML, Gao S, Ni J, Zhou LX, Yao M, et al. In vivo high-resolution MR imaging of symptomatic and asymptomatic middle cerebral artery atherosclerotic stenosis. *Atherosclerosis* 2010;212:507-511.
47. Schoenhagen P, Ziada KM, Kapadia SR, Crowe TD, Nissen SE, Tuzcu EM. Extent and direction of arterial remodeling in stable versus unstable coronary syndromes: an intravascular ultrasound study. *Circulation* 2000;101:598-603.
48. Varnava AM, Mills PG, Davies MJ. Relationship between coronary artery remodeling and plaque vulnerability. *Circulation* 2002;105:939-943.
49. Tsukahara T, Minematsu K. Overview of spontaneous cervicocephalic arterial dissection in Japan. *Acta Neurochir Suppl* 2010;107:35-40.
50. Arauz A, Ruiz A, Pacheco G, Rojas P, Rodriguez-Armida M, Cantu C, et al. Aspirin versus anticoagulation in intra- and extracranial vertebral artery dissection. *Eur J Neurol* 2013;20:

167-172.
51. Guillon B, Levy C, Bousser MG. Internal carotid artery dissection: an update. *J Neurol Sci* 1998;153:146-158.
52. Maruyama H, Nagoya H, Kato Y, Deguchi I, Fukuoka T, Ohe Y, et al. Spontaneous cervicocephalic arterial dissection with headache and neck pain as the only symptom. *J Headache Pain* 2012;13:247-253.
53. Han M, Rim NJ, Lee JS, Kim SY, Choi JW. Feasibility of high-resolution MR imaging for the diagnosis of intracranial vertebrobasilar artery dissection. *Eur Radiol* 2014;24:3017-3024.
54. Gao PH, Yang L, Wang G, Guo L, Liu X, Zhao B. Symptomatic unruptured isolated middle cerebral artery dissection: clinical and magnetic resonance imaging features. *Clin Neuroradiol* 2014. [Epub ahead of print].
55. Kwak HS, Hwang SB, Chung GH, Jeong SK. High-resolution magnetic resonance imaging of symptomatic middle cerebral artery dissection. *J Stroke Cerebrovasc Dis* 2014;23:550-553.
56. Pfefferkorn T, Saam T, Rominger A, Habs M, Gerdes LA, Schmidt C, et al. Vessel wall inflammation in spontaneous cervical artery dissection: a prospective, observational positron emission tomography, computed tomography, and magnetic resonance imaging study. *Stroke* 2011;42:1563-1568.
57. Sakurai K, Miura T, Sagisaka T, Hattori M, Matsukawa N, Mase M, et al. Evaluation of luminal and vessel wall abnormalities in subacute and other stages of intracranial vertebrobasilar artery dissections using the volume isotropic turbo-spin-echo acquisition (VISTA) sequence: a preliminary study. *J Neuroradiol* 2013;40:19-28.
58. Yoon W, Seo JJ, Kim TS, Do HM, Jayaraman MV, Marks MP. Dissection of the V4 segment of the vertebral artery: clinicoradiologic manifestations and endovascular treatment. *Eur Radiol* 2007;17:983-993.
59. Naim C, Douziech M, Therasse E, Robillard P, Giroux MF, Arsenault F, et al. Vulnerable atherosclerotic carotid plaque evaluation by ultrasound, computed tomography angiography, and magnetic resonance imaging: an overview. *Can Assoc Radiol J* 2014;65:275-286.
60. Mizutani T. Natural course of intracranial arterial dissections. *J Neurosurg* 2011;114:1037-1044.
61. Kim BM, Kim SH, Kim DI, Shin YS, Suh SH, Kim DJ, et al. Outcomes and prognostic factors of intracranial unruptured vertebrobasilar artery dissection. *Neurology* 2011;76:1735-1741.
62. Arauz A, Marquez JM, Artigas C, Balderrama J, Orrego H. Recanalization of vertebral artery dissection. *Stroke* 2010;41:717-721.
63. Tan TY, Kuo YL, Lin WC, Chen TY. Effect of lipid-lowering therapy on the progression of intracranial arterial stenosis. *J Neurol* 2009;256:187-193.
64. Kwon SU, Cho YJ, Koo JS, Bae HJ, Lee YS, Hong KS, et al. Cilostazol prevents the progression of the symptomatic intracranial arterial stenosis: the multicenter double-blind placebo-controlled trial of cilostazol in symptomatic intracranial arterial stenosis. *Stroke* 2005;36:782-786.
65. Habs M, Pfefferkorn T, Cyran CC, Grimm J, Rominger A, Hacker M, et al. Age determination of vessel wall hematoma in spontaneous cervical artery dissection: a multi-sequence 3T cardiovascular magnetic resonance study. *J Cardiovasc Magn Reson* 2011;13:76.
66. Suzuki J, Takaku A. Cerebrovascular "moyamoya" disease: disease showing abnormal net-like vessels in base of brain. *Arch Neurol* 1969;20:288-299.
67. Scott RM, Smith ER. Moyamoya disease and moyamoya syndrome. *N Engl J Med* 2009;360:1226-1237.
68. Achrol AS, Guzman R, Lee M, Steinberg GK. Pathophysiology and genetic factors in moyamoya disease. *Neurosurg Focus* 2009;26:E4.
69. Fujimura M, Sonobe S, Nishijima Y, Niizuma K, Sakata H, Kure S, et al. Genetics and biomarkers of moyamoya disease: significance of RNF213 as a susceptibility gene. *J Stroke* 2014;16:65-72.
70. Yuan M, Liu ZQ, Wang ZQ, Li B, Xu LJ, Xiao XL. High-resolution MR imaging of the arterial wall in moyamoya disease. *Neurosci Lett* 2015;584:77-82.
71. Kim YJ, Lee DH, Kwon JY, Kang DW, Suh DC, Kim JS, et al. High resolution MRI difference between moyamoya disease and intracranial atherosclerosis. *Eur J Neurol* 2013;20:1311-1318.
72. Hui FK, Zhu X, Jones SE, Uchino K, Bullen JA, Hussain MS, et al. Early experience in high-resolution MRI for large vessel occlusions. *J Neurointerv Surg* 2015;7:509-516.
73. Kim SM, Ryu CW, Jahng GH, Kim EJ, Choi WS. Two different morphologies of chronic unilateral middle cerebral artery occlusion: evaluation using high-resolution MRI. *J Neuroimaging* 2014;24:460-466.
74. Salvarani C, Brown RD Jr, Calamia KT, Christianson TJ, Weigand SD, Miller DV, et al. Primary central nervous system vasculitis: analysis of 101 patients. *Ann Neurol* 2007;62:442-451.
75. Hajj-Ali RA, Calabrese LH. Diagnosis and classification of central nervous system vasculitis. *J Autoimmun* 2014;48-49:149-152.
76. Calabrese LH, Mallek JA. Primary angiitis of the central nervous system. Report of 8 new cases, review of the literature, and proposal for diagnostic criteria. *Medicine (Baltimore)* 1988;67:20-39.
77. Obusez EC, Hui F, Hajj-Ali RA, Cerejo R, Calabrese LH, Hammad T, et al. High-resolution MRI vessel wall imaging: spatial

http://dx.doi.org/10.5853/jos.2015.17.3.238

and temporal patterns of reversible cerebral vasoconstriction syndrome and central nervous system vasculitis. *AJNR Am J Neuroradiol* 2014;35:1527-1532.
78. Gomes LJ. The role of imaging in the diagnosis of central nervous system vasculitis. *Curr Allergy Asthma Rep* 2010;10:163-170.
79. Kuker W, Gaertner S, Nagele T, Dopfer C, Schoning M, Fiehler J, et al. Vessel wall contrast enhancement: a diagnostic sign of cerebral vasculitis. *Cerebrovasc Dis* 2008;26:23-29.
80. Saam T, Habs M, Pollatos O, Cyran C, Pfefferkorn T, Dichgans M, et al. High-resolution black-blood contrast-enhanced T1 weighted images for the diagnosis and follow-up of intracranial arteritis. *Br J Radiol* 2010;83:e182-184.
81. Serdaru M, Chiras J, Cujas M, Lhermitte F. Isolated benign cerebral vasculitis or migrainous vasospasm? *J Neurol Neurosurg Psychiatry* 1984;47:73-76.
82. Hajj-Ali RA, Furlan A, Abou-Chebel A, Calabrese LH. Benign angiopathy of the central nervous system: cohort of 16 patients with clinical course and long-term followup. *Arthritis Rheum* 2002;47:662-669.
83. Calabrese LH, Dodick DW, Schwedt TJ, Singhal AB. Narrative review: reversible cerebral vasoconstriction syndromes. *Ann Intern Med* 2007;146:34-44.
84. Mandell DM, Matouk CC, Farb RI, Krings T, Agid R, terBrugge K, et al. Vessel wall MRI to differentiate between reversible cerebral vasoconstriction syndrome and central nervous system vasculitis: preliminary results. *Stroke* 2012;43:860-862.
85. Findlay JM, Weir BK, Kanamaru K, Espinosa F. Arterial wall changes in cerebral vasospasm. *Neurosurgery* 1989;25:736-745.
86. Kan P, Mokin M, Dumont TM, Snyder KV, Siddiqui AH, Levy EI, et al. Cervical carotid artery stenosis: latest update on diagnosis and management. *Curr Probl Cardiol* 2012;37:127-169.
87. Faries PL, Chaer RA, Patel S, Lin SC, DeRubertis B, Kent KC. Current management of extracranial carotid artery disease. *Vasc Endovascular Surg* 2006;40:165-175.
88. Fine-Edelstein JS, Wolf PA, O'Leary DH, Poehlman H, Belanger AJ, Kase CS, et al. Precursors of extracranial carotid atherosclerosis in the Framingham Study. *Neurology* 1994;44:1046-1050.
89. Rockman CB, Jacobowitz GR, Gagne PJ, Adelman MA, Lamparello PJ, Landis R, et al. Focused screening for occult carotid artery disease: patients with known heart disease are at high risk. *J Vasc Surg* 2004;39:44-51.
90. Barnett HJ, Taylor DW, Eliasziw M, Fox AJ, Ferguson GG, Haynes RB, et al. Benefit of carotid endarterectomy in patients with symptomatic moderate or severe stenosis. North American Symptomatic Carotid Endarterectomy Trial Collaborators. *N Engl J Med* 1998;339:1415-1425.
91. Group ECSTC. Randomised trial of endarterectomy for recently symptomatic carotid stenosis: final results of the MRC European Carotid Surgery Trial (ECST). *The Lancet* 1998;351:1379-1387.
92. Saba L, Mallarini G. A comparison between NASCET and ECST methods in the study of carotids: Evaluation using Multi-Detector-Row CT angiography. *Eur J Radiol* 2010;76:42-47.
93. Lovett J, Gallagher P, Rothwell P. Reproducibility of histological assessment of carotid plaque: implications for studies of carotid imaging. *Cerebrovasc Dis (Basel, Switzerland)* 2003;18:117-123.
94. Wasserman BA. Advanced contrast-enhanced MRI for looking beyond the lumen to predict stroke: building a risk profile for carotid plaque. *Stroke* 2010;41:S12-16.
95. Wasserman BA, Wityk RJ, Trout HH 3rd, Virmani R. Low-grade carotid stenosis: looking beyond the lumen with MRI. *Stroke* 2005;36:2504-2513.
96. Kullo IJ, Edwards WD, Schwartz RS. Vulnerable plaque: pathobiology and clinical implications. *Ann Int Med* 1998;129:1050-1060.
97. Saam T, Cai J, Ma L, Cai Y-Q, Ferguson MS, Polissar NL, et al. Comparison of symptomatic and asymptomatic atherosclerotic carotid plaque features with in vivo MR imaging. *Radiology* 2006;240:464-472.
98. Mokhtari-Dizaji M, Montazeri M, Saberi H. Differentiation of mild and severe stenosis with motion estimation in ultrasound images. *Ultrasound Med Biol* 2006;32:1493-1498.
99. Bluth EI, Sunshine JH, Lyons JB, Beam CA, Troxclair LA, Althans-Kopecky L, et al. Power Doppler imaging: initial evaluation as a screening examination for carotid artery stenosis. *Radiology* 2000;215:791-800.
100. Grant EG, Benson CB, Moneta GL, Alexandrov AV, Baker JD, Bluth EI, et al. Carotid artery stenosis: gray-scale and Doppler US diagnosis—Society of Radiologists in Ultrasound Consensus Conference. *Radiology* 2003;229:340-346.
101. Heijenbrok-Kal MH, Buskens E, Nederkoorn PJ, van der Graaf Y, Hunink MG. Optimal peak systolic velocity threshold at duplex us for determining the need for carotid endarterectomy: a decision analytic approach. *Radiology* 2006;238:480-488.
102. Saba L, Sanfilippo R, Montisci R, Mallarini G. Correlation between US-PSV and MDCTA in the quantification of carotid artery stenosis. *Eur J Radiol* 2010;74:99-103.
103. Kitamura A, Iso H, Imano H, Ohira T, Okada T, Sato S, et al. Carotid intima-media thickness and plaque characteristics as a risk factor for stroke in Japanese elderly men. *Stroke* 2004;35:2788-2794.
104. Prabhakaran S, Rundek T, Ramas R, Elkind MS, Paik MC,

Boden-Albala B, et al. Carotid plaque surface irregularity predicts ischemic stroke: the northern Manhattan study. *Stroke* 2006;37:2696-2701.
105. Mathiesen EB, Bonaa KH, Joakimsen O. Echolucent plaques are associated with high risk of ischemic cerebrovascular events in carotid stenosis: the Tromsø study. *Circulation* 2001;103:2171-2175.
106. Polak JF, Shemanski L, O'Leary DH, Lefkowitz D, Price TR, Savage PJ, et al. Hypoechoic plaque at US of the carotid artery: an independent risk factor for incident stroke in adults aged 65 years or older. Cardiovascular Health Study. *Radiology* 1998;208:649-654.
107. Halliday A, Mansfield A, Marro J, Peto C, Peto R, Potter J, et al. Prevention of disabling and fatal strokes by successful carotid endarterectomy in patients without recent neurological symptoms: randomised controlled trial. *Lancet* 2004;363:1491-1502.
108. Lorenz MW, von Kegler S, Steinmetz H, Markus HS, Sitzer M. Carotid intima-media thickening indicates a higher vascular risk across a wide age range: prospective data from the Carotid Atherosclerosis Progression Study (CAPS). *Stroke* 2006;37:87-92.
109. Koelemay MJ, Nederkoorn PJ, Reitsma JB, Majoie CB. Systematic review of computed tomographic angiography for assessment of carotid artery disease. *Stroke* 2004;35:2306-2312.
110. Saba L, Caddeo G, Sanfilippo R, Montisci R, Mallarini G. CT and ultrasound in the study of ulcerated carotid plaque compared with surgical results: potentialities and advantages of multidetector row CT angiography. *AJNR Am J Neuroradiol* 2007;28:1061-1066.
111. Schroeder S, Kopp AF, Baumbach A, Meisner C, Kuettner A, Georg C, et al. Noninvasive detection and evaluation of atherosclerotic coronary plaques with multislice computed tomography. *J Am Coll Cardiol* 2001;37:1430-1435.
112. Saba L, Caddeo G, Sanfilippo R, Montisci R, Mallarini G. Efficacy and sensitivity of axial scans and different reconstruction methods in the study of the ulcerated carotid plaque using multidetector-row CT angiography: comparison with surgical results. *AJNR Am J Neuroradiol* 2007;28:716-723.
113. Hayes CE, Mathis CM, Yuan C. Surface coil phased arrays for high-resolution imaging of the carotid arteries. *J Magn Reson Imaging* 1996;6:109-112.
114. Underhill HR, Yarnykh VL, Hatsukami TS, Wang J, Balu N, Hayes CE, et al. Carotid plaque morphology and composition: initial comparison between 1.5- and 3.0-T magnetic field strengths. *Radiology* 2008;248:550-560.
115. Toussaint JF, LaMuraglia GM, Southern JF, Fuster V, Kantor HL. Magnetic resonance images lipid, fibrous, calcified, hemorrhagic, and thrombotic components of human atherosclerosis in vivo. *Circulation* 1996;94:932-938.
116. Cai J, Hatsukami TS, Ferguson MS, Kerwin WS, Saam T, Chu B, et al. In vivo quantitative measurement of intact fibrous cap and lipid-rich necrotic core size in atherosclerotic carotid plaque: comparison of high-resolution, contrast-enhanced magnetic resonance imaging and histology. *Circulation* 2005;112:3437-3444.
117. Chu B, Kampschulte A, Ferguson MS, Kerwin WS, Yarnykh VL, O'Brien KD, et al. Hemorrhage in the atherosclerotic carotid plaque: a high-resolution MRI study. *Stroke* 2004;35:1079-1084.
118. Corti R, Fuster V, Fayad ZA, Worthley SG, Helft G, Chaplin WF, et al. Effects of aggressive versus conventional lipid-lowering therapy by simvastatin on human atherosclerotic lesions: a prospective, randomized, double-blind trial with high-resolution magnetic resonance imaging. *J Am Coll Cardiol* 2005;46:106-112.
119. Yuan C, Mitsumori LM, Ferguson MS, Polissar NL, Echelard D, Ortiz G, et al. In vivo accuracy of multispectral magnetic resonance imaging for identifying lipid-rich necrotic cores and intraplaque hemorrhage in advanced human carotid plaques. *Circulation* 2001;104:2051-2056.
120. Farb A, Burke AP, Tang AL, Liang TY, Mannan P, Smialek J, et al. Coronary plaque erosion without rupture into a lipid core: a frequent cause of coronary thrombosis in sudden coronary death. *Circulation* 1996;93:1354-1363.
121. Morrisett J, Vick W, Sharma R, Lawrie G, Reardon M, Ezell E, et al. Discrimination of components in atherosclerotic plaques from human carotid endarterectomy specimens by magnetic resonance imaging ex vivo. *Magn Reson Imaging* 2003;21:465-474.
122. Watanabe Y, Nagayama M. MR plaque imaging of the carotid artery. *Neuroradiology* 2010;52:253-274.
123. Maynor CH, Charles HC, Herfkens RJ, Suddarth SA, Johnson GA. Chemical shift imaging of atherosclerosis at 7.0 Tesla. *Invest Radiol* 1989;24:52-60.
124. Serfaty JM, Chaabane L, Tabib A, Chevallier JM, Briguet A, Douek PC. Atherosclerotic plaques: classification and characterization with T2-weighted high-spatial-resolution MR imaging—an in vitro study. *Radiology* 2001;219:403-410.
125. Bitar R, Moody AR, Leung G, Symons S, Crisp S, Butany J, et al. In vivo 3D high-spatial-resolution MR imaging of intraplaque hemorrhage. *Radiology* 2008;249:259-267.
126. Yim YJ, Choe YH, Ko Y, Kim ST, Kim KH, Jeon P, et al. High signal intensity halo around the carotid artery on maximum intensity projection images of time-of-flight MR angiography: a new sign for intraplaque hemorrhage. *J Magn Reson Imaging*

http://dx.doi.org/10.5853/jos.2015.17.3.238

2008;27:1341-1346.

127. Touze E, Toussaint JF, Coste J, Schmitt E, Bonneville F, Vandermarcq P, et al. Reproducibility of high-resolution MRI for the identification and the quantification of carotid atherosclerotic plaque components: consequences for prognosis studies and therapeutic trials. *Stroke* 2007;38:1812-1819.
128. Howarth SP, Tang TY, Trivedi R, Weerakkody R, U-King-Im J, Gaunt ME, et al. Utility of USPIO-enhanced MR imaging to identify inflammation and the fibrous cap: a comparison of symptomatic and asymptomatic individuals. *Eur J Radiol* 2009;70:555-560.
129. Sheikine Y, Akram K. FDG-PET imaging of atherosclerosis: do we know what we see? *Atherosclerosis* 2010;211:371-380.
130. Rohren EM, Turkington TG, Coleman RE. Clinical applications of PET in oncology. *Radiology* 2004;231:305-332.
131. Müller HFG, Viaccoz A, Fisch L, Bonvin C, Lovblad K-O, Ratib O, et al. 18FDG-PET-CT: an imaging biomarker of high-risk carotid plaques. Correlation to symptoms and microembolic signals. *Stroke* 2014;45:3561-3566.
132. Rudd JHF, Warburton EA, Fryer TD, Jones HA, Clark JC, Antoun N, et al. Imaging atherosclerotic plaque inflammation with F-18-fluorodeoxyglucose positron emission tomography. *Circulation* 2002;105:2708-2711.
133. Lederman RJ, Raylman RR, Fisher SJ, Kison PV, San H, Nabel EG, et al. Detection of atherosclerosis using a novel positron-sensitive probe and 18-fluorodeoxyglucose (FDG). *Nucl Med Commun* 2001;22:747-753.